

ATLAS Level-1 Endcap Muon Trigger for Run 3

Tomoe Kishimoto*, on behalf of the ATLAS collaboration

International Center for Elementary Particle Physics, The University of Tokyo

E-mail: Tomoe.Kishimoto@cern.ch

The Level-1 endcap muon trigger in the ATLAS experiment is a hardware trigger system for the endcap region. The system identifies bunch crossings with muon candidates of high transverse momentum by combining information from fast-response muon detectors. The Large Hadron Collider at CERN is scheduled to start the physics data-taking from 2021 as Run 3. An upgrade program of the Level-1 endcap muon trigger for Run 3 is required to reduce backgrounds in the muon trigger candidates. New muon detectors called New Small Wheel, and RPC-BIS78 will be installed to improve detector coverages and transverse momentum resolution. Thus, a new trigger processor board called Sector Logic has been developed to handle information from the new detectors. This paper describes the upgrade program of the Level-1 endcap muon trigger, particularly emphasizing on the new algorithm on Sector Logic board as well as the expected trigger performance.

*European Physical Society Conference on High Energy Physics - EPS-HEP2019 -
10-17 July, 2019
Ghent, Belgium*

*Speaker.

1. Introduction

Muons in the final states are distinctive signatures of various physics studies at the ATLAS experiment [1], such as the measurements of the Higgs boson couplings and searches for new phenomena. Thus, a highly efficient muon trigger is one of the key components to improve the acceptance of many interesting physics processes.

The ATLAS muon trigger system selects events in two steps. The signals from fast-response muon detectors are processed by custom-made hardware to reconstruct muon track candidates, and they are sent to the central trigger processor to make the Level-1 (L1) trigger decisions. The L1 muon trigger system has multiple transverse momentum (p_T) thresholds to select the muon candidate. In addition, the L1 trigger carries the position information where muon candidates are found (Region of Interest, RoI). In the later step, software-based High-Level Trigger (HLT) reconstructs tracks in the vicinity of the RoI given by the L1 trigger and makes final trigger decisions. The Resistive Plate Chambers (RPC) and Thin Gap Chambers (TGC) are used in the L1 trigger system to detect muons in the barrel region ($|\eta| \leq 1.05$) and the endcap region ($1.05 < |\eta| < 2.4$), respectively [2].

The Large Hadron Collider (LHC) at CERN is scheduled to start the physics data-taking from 2021 as Run 3. An upgrade program of the L1 endcap muon trigger is required to improve trigger performances for Run 3, especially to reject fake triggers due to slow particles originating from the endcap toroid magnet or shielding. The new muon detectors called New Small Wheel (NSW) [3], and RPC-BIS78 [4] will be installed as a part of the upgrade. They will provide a better coverage for trigger coincidences and precision measurements of muon track segments. Therefore, new trigger processor board called New Sector Logic (NSL) was developed to handle information from the new detectors.

This paper describes the upgrade program of the L1 endcap muon trigger, particularly emphasizing on the new algorithm in the NSL as well as the expected trigger performance. The paper is organized as follows. The status and performance of the L1 endcap muon trigger during Run 2 is reported in Section 2. An overview of the upgrade program for Run 3 is given in Section 3. The design of the NSL board is described in Section 4, followed by a description of the coincidence algorithm on the NSL and its performances in Section 5. Muon charge identification performance at the L1 endcap muon trigger is shown in Section 6. Results of the trigger rate estimation for Run 3 are shown in Section 7. Finally, the conclusion is presented in Section 8.

2. Status and performance of the L1 endcap muon trigger in Run 2

Figure 1 (a) shows a section view of the L1 muon trigger system. Three stations of the TGC Big Wheel (TGC-BW) were used in the L1 endcap muon trigger in Run 1 (2010–2012). Additional inputs from the TGC inner stations (TGC-EI/FI) and the Tile calorimeter [5] were introduced for taking coincidences with TGC-BW, and those coincidences successfully reduced the fake triggers in Run 2 (2016–2018). Figure 1 (b) shows the efficiencies for the L1 endcap muon trigger in 2018 as a function of p_T of the offline-reconstructed muon. The trigger efficiencies in the plateau region were about 90% with stable operation. The p_T threshold of the primary L1 single-muon trigger

was 20 GeV (L1_MU20). The trigger rate of L1_MU20 was about 17 kHz with an instantaneous luminosity at $L = 2 \times 10^{34} \text{ cm}^{-2}\text{s}^{-1}$ for the entire barrel and endcap regions.

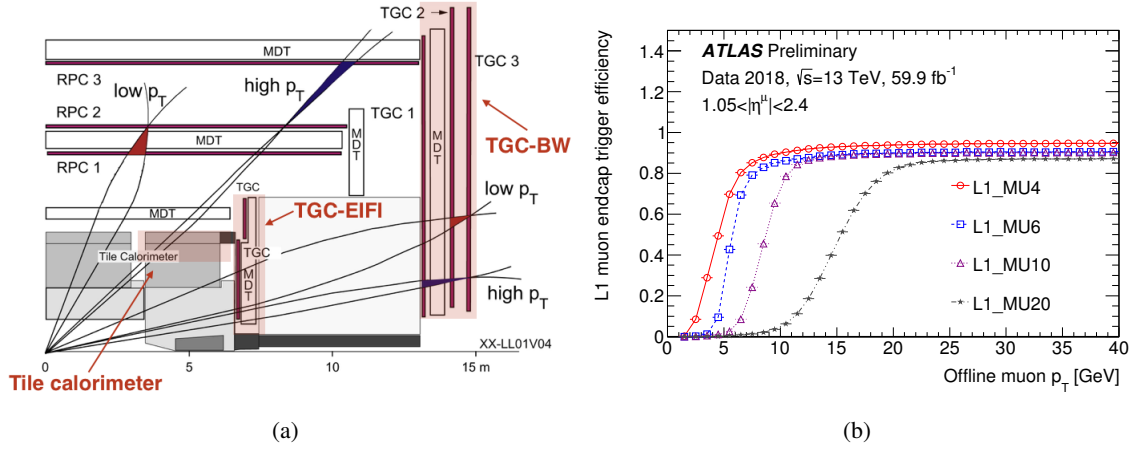


Figure 1: (a) A section view of the L1 muon trigger system. The TGC-BW, TGC-EI/FI and the Tile calorimeter were used for the L1 endcap muon trigger in Run 2. (b) The efficiencies for L1 single-muon triggers as a function of the transverse momentum of the offline-reconstructed muon in the endcap region in 2018 [6].

Figure 2 shows the η distributions of RoIs by L1_MU20 in 2017. It can be confirmed that there are large entries in the endcap regions compared to the barrel region. The blue histogram shows the L1 muon trigger candidates that are not associated with offline-reconstructed muons. The red histogram shows the L1 muon trigger candidates that are associated with the offline-reconstructed muons with p_T of less than 20 GeV. The upgrade program for Run 3 aims at reducing the trigger rate by eliminating these contaminations.

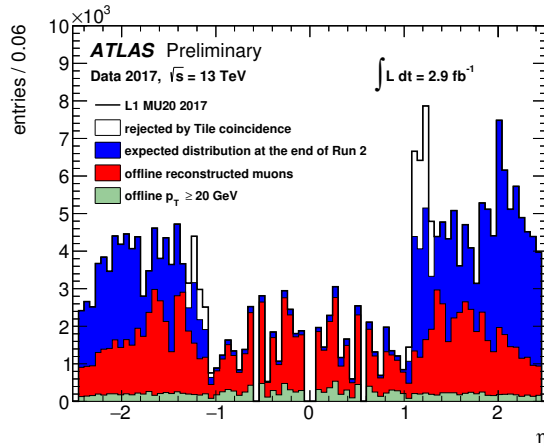


Figure 2: Distributions of η for L1_MU20 in 2017 [6]. The expected distribution at the end of Run 2 after enabling TGC-EI/FI and Tile calorimeter coincidences is also shown.

3. Overview of the L1 endcap muon trigger upgrade program for Run 3

The objective of the upgrade for the L1 endcap muon trigger system is to reduce trigger rates by introducing new coincidences. There was a significant contribution from background events. As shown in Figure 2, the backgrounds are:

- slow particles originating from the endcap toroid magnets or shieldings,
- low- p_T muons below the threshold due to the limited p_T resolution at the L1 trigger.

New muon detectors will be installed into the inner regions before the endcap toroid magnet for Run 3 to reduce both the background sources. The Small Wheel in Run 2, which consists of TGC, Monitored Drift Chamber (MDT) [2] and Cathode Strip Chamber (CSC) [2] will be replaced with the NSW. The NSW consists of small-strip TGC (sTGC) and Micromegas (MM) detectors [3]. The NSW will be able to provide a better coverage up to $|\eta| = 2.4$, and precision measurements of muon track segments. New RPC detectors (RPC-BIS78) will be installed to the edge of the barrel muon trigger system for the precision measurements of muon track positions in the barrel-endcap transition region. New trigger coincidences between TGC-BW and NSW/RPC-BIS78 will be introduced to reject the fake triggers and improve the muon p_T resolution.

A new electronics, NSL board, has been developed to handle information from the new detectors. The NSL board reconstructs muon track candidates using the dedicated algorithm based on data received from the legacy detectors (TGC-BW, TGC-EI and Tile calorimeter) and the new detectors (NSW and RPC-BIS78). Figure 3 shows an overview of the L1 endcap muon trigger system for Run 3, which focuses on the TGC-BW and NSW. The TGC-BW provides the hit position at the BW3 station (η_{BW} , ϕ_{BW}) and the difference of the hit position at BW1 station with respect to the position pointing to the interaction point (ΔR , $\Delta\Phi$). The NSW provides the position of the track segment (η_{NSW} , ϕ_{NSW}) and the angle difference between the direction of the reconstructed segment and that extrapolated back to the interaction point ($\Delta\theta$). The NSL uses this information to reconstruct muon track candidates and sends results to the central trigger processor.

4. New Sector Logic board

The NSL board has a Xilinx Kintex7 FPGA to make use of Multi-Gigabit transceiver technology (GTX) [7]. The FPGA (Xilinx Kintex7 XC7K410T) on the NSL board provides twenty times larger resources compared to that used in Run 2 (Xilinx VirtexII VC2V3000 or VirtexII VC2V1000). The NSL board has 12 GTX interfaces and 14 G-Link [8] receivers. The GTX interfaces will be used to receive the data from the NSW, RPC-BIS78, Tile calorimeter and TGC-EI, and send the muon track candidates to the central trigger processor. The G-Link receivers will be used to receive the data from the legacy TGC-BW. 72 NSL boards will be required for the whole L1 endcap muon trigger system. All the NSL boards have been produced and installed to the ATLAS counting room.

5. Coincidence algorithm and performance

The algorithm on the NSL uses the information from several sub-detectors to reconstruct muon track candidates as discussed in Section 3. This section describes the coincidence algorithm and

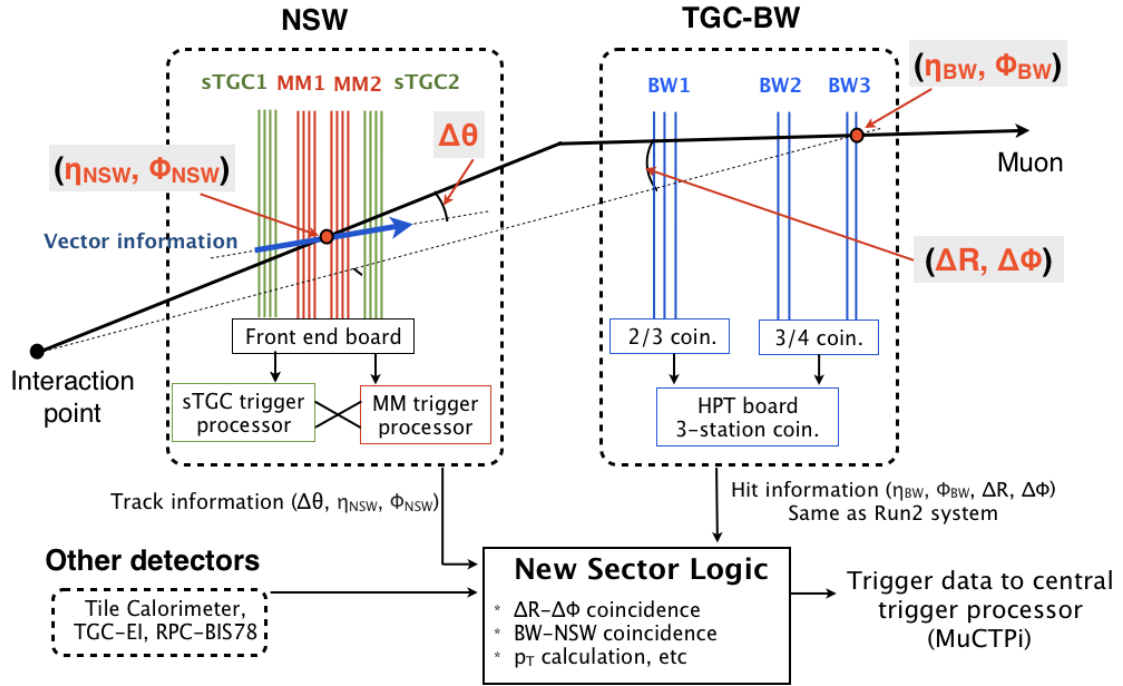


Figure 3: An overview of the L1 endcap muon trigger system for Run 3.

the performance with a focus on the coincidence with the NSW because the NSW will provide a significant improvement of the performance of L1 endcap muon trigger.

The muon candidates in $|\eta| > 1.3$ which satisfied the legacy TGC-BW local coincidence [9] are required to pass the additional algorithm using the NSW information. There are several baseline ideas of the algorithm for the TGC-BW and NSW coincidence. The position and angular correlations between the TGC-BW and NSW will be used for the coincidence algorithm. Figure 4 shows the distributions of position differences between the trigger seed on BW3 (η_{BW} and Φ_{BW}) and track segment in NSW (η_{NSW} and Φ_{NSW}) in a Monte Carlo simulation. Single muons with positive and negative charge were generated in the simulation. It can be confirmed that the distribution varies depending on the muon p_T . Look-Up-Tables (LUT), which are implemented to the FPGA, are defined based on these position patterns using the simulation for different muon p_T thresholds. The correlation between the deviations and the muon p_T is quite different depending on the position because the toroidal magnetic field is not uniform. Thus, the LUTs are defined depending on the position to maximize the performance. Another coincidence using the angular correlation between $\Delta\theta$ and η_{BW} will also be applied using LUTs.

The performances of the TGC-BW and NSW coincidence using the LUTs have been estimated using simulation. Figure 5 (a) shows the relative trigger efficiencies with respect to the Run 2 system by introducing the NSW coincidence for L1_MU20. It can be seen that the trigger efficiencies for the low- p_T muons below the threshold are reduced effectively by taking the coincidence. Only a few percents trigger efficiency loss is expected because of the NSW track reconstruction efficiency. Figure 5 (b) shows the p_T distributions of offline-reconstructed muons associated with

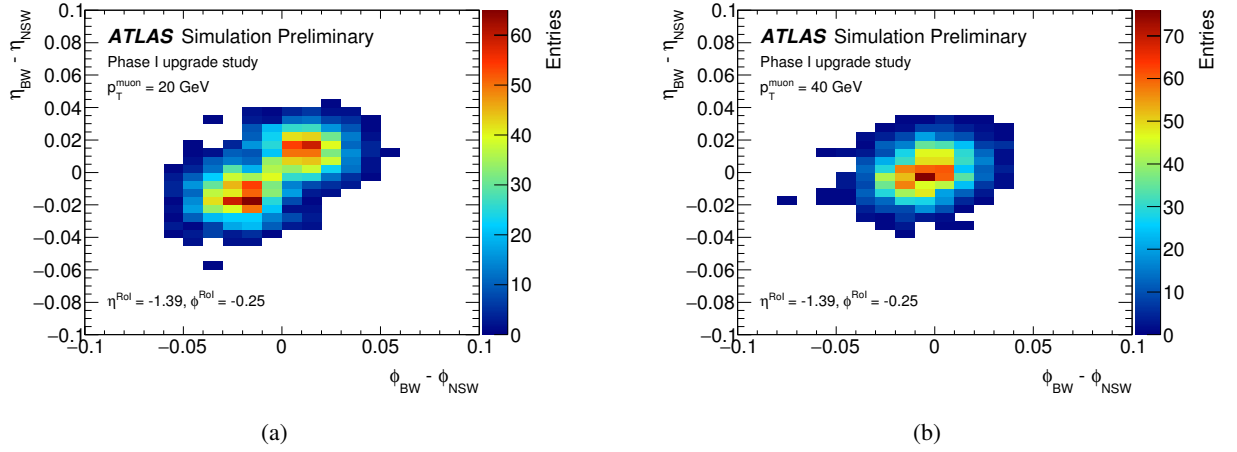


Figure 4: The distributions of position differences between the TGC-BW and NSW [6]. The distributions are obtained by simulation with muon $p_T = 20$ GeV (a) and 40 GeV (b), respectively. The position resolution of $\eta_{NSW} = 0.005$ and $\Phi_{NSW} = 0.01$ and the angle resolution of $\Delta\theta = 0.001$ are assumed in this simulation. Two peaks are observed in the distribution with muon $p_T = 20$ GeV since the position differences depend on muon charge.

L1_MU20 in Run 2 data. The figure also shows the expected p_T distributions by introducing the NSW coincidences. For example, about 50% reduction is expected at offline-reconstructed muon $p_T = 10$ GeV.

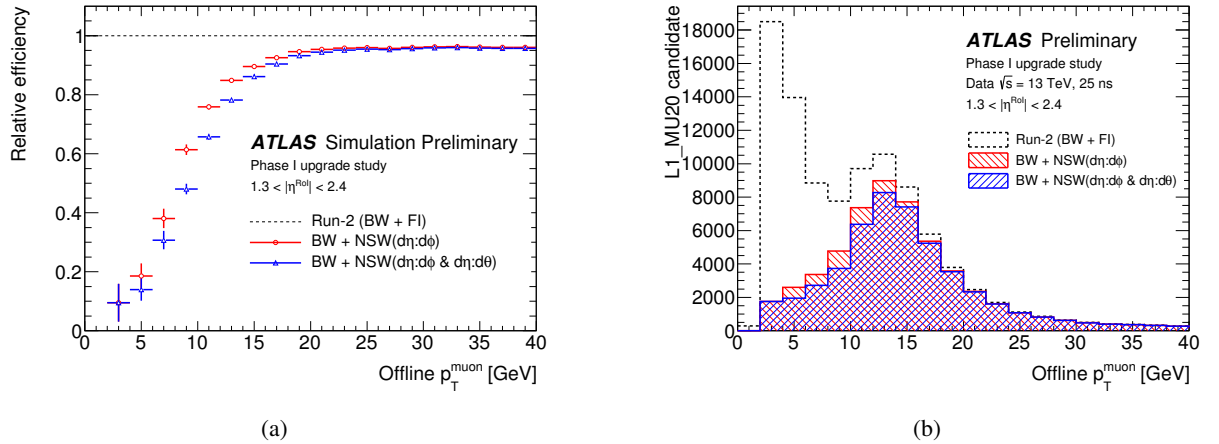


Figure 5: (a) The relative trigger efficiencies for L1_MU20 by introducing the NSW coincidence [6]. (b) The p_T distributions of offline-reconstructed muons associated with L1_MU20 by introducing the NSW coincidence [6].

6. Muon charge identification

The L1 endcap muon trigger has a capability of identifying muon charges by measuring the bending direction in the magnetic field, as illustrated in Figure 6 (a). Several applications in the L1 trigger benefit by the charge information, such as the topological triggers for low- p_T di-muons.

Dedicated LUTs for identifying the muon charge will be allowed to implement to the NSL board thanks to the new FPGA resources. The accuracy of the muon charge identification at the L1 endcap muon trigger is estimated using simulation. Figure 6 (b) shows the estimated impact of the accuracy on the trigger efficiency. The red triangles show the trigger efficiency with 4 GeV of p_T threshold (L1_MU4) in terms of the truth muon p_T . The blue triangles show the trigger efficiency of L1_MU4 with correctly identified charge. The L1_MU4 is the lowest threshold muon trigger in Run 2. It can be confirmed that the efficiencies of correctly identifying charge are greater than 98% up to $p_T = 30$ GeV. The efficiency gets worse with increasing muon p_T , but the use cases focus on the low- p_T muons.

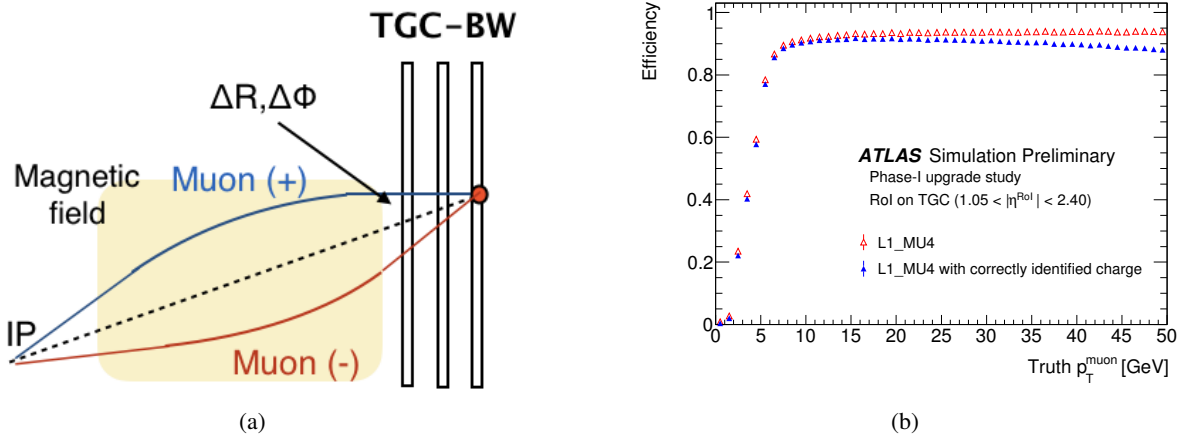


Figure 6: (a) An illustration of the charge identification at the L1 endcap muon trigger. (b) The expected trigger efficiency of the L1 endcap muon trigger with 4 GeV of p_T threshold (L1_MU4) in Run 3 [6]. The figure also shows the trigger efficiency of L1_MU4 with correctly identified charge.

7. Trigger rate estimation for Run 3

The expected trigger rate by introducing the new coincidences are estimated using Run 2 real data. The data with L1_MU20 candidates collected by HLT pass-through triggers not requiring any HLT algorithms are used for the estimation. MDT track segments in the data are used to emulate the NSW and RPC-BIS78 track segments. The LUTs, which are discussed in Section 5, are applied to estimate the number of muon track candidates. The LUTs for the RPC-BIS78 coincidence are also defined based on the hit position correlation and are used in the estimation. Figure 7 shows the expected η distributions of L1_MU20 for Run 3. It can be confirmed that about 90% of the fake triggers are rejected by the new coincidences. The low- p_T muon candidates are also reduced thanks to the fine granularity of the NSW and RPC-BIS78. The simulation confirmed that the trigger rate of L1_MU20 will be reduced by about 45% compared to the Run 2 system.

8. Conclusion

The upgrade program of the L1 endcap muon trigger for Run 3 is aimed at reducing the fake triggers and low- p_T muons below the thresholds. The new detectors, NSW and RPC-BIS78, will

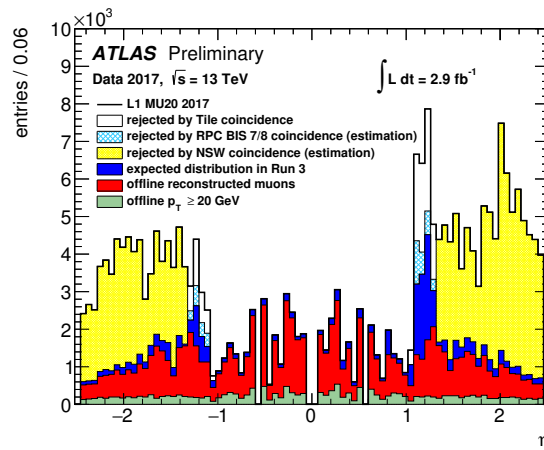


Figure 7: The expected η distributions of L1_MU20 for Run 3 [6]. The expected distribution in Run 3 shows the distribution after enabling all coincidences by the Tile calorimeter, RPC BIS78 and NSW.

be installed to the inner region of the ATLAS detector to reduce both the background sources. The NSL boards have been produced to handle the data from the new detectors. The new algorithm on the NSL has been developed to perform the coincidences between the TGC-BW and NSW. The simulation confirmed that the trigger rate of L1_MU20 will be reduced by about 45% compared to the Run 2 system by introducing the new coincidences.

References

- [1] ATLAS Collaboration, *The ATLAS Experiment at the CERN Large Hadron Collider*, JINST 3 (2008) S08003.
- [2] ATLAS Collaboration, *ATLAS muon spectrometer: Technical Design Report*, ATLAS-TDR-10 [<https://cds.cern.ch/record/331068>].
- [3] ATLAS Collaboration, *New Small Wheel Technical Design Report*, ATLAS-TDR-020 [<https://cds.cern.ch/record/1552862/>].
- [4] ATLAS Muon Collaboration, *Proposal of upgrade of the ATLAS muon trigger in the Barrel - End Cap transition region with RPCs*, PoS TIPP2014, 2014, p. 117.
- [5] ATLAS Collaboration, *ATLAS tile calorimeter: Technical Design Report*, ATLAS-TDR-3 [<https://cds.cern.ch/record/331062/>].
- [6] L1 Muon Public Results, [<https://twiki.cern.ch/twiki/bin/view/AtlasPublic/L1MuonTriggerPublicResults>].
- [7] 7 Series FPGAs GTX/GTH Transceivers User Guide [https://www.xilinx.com/support/documentation/user_guides/ug476_7Series_Transceivers.pdf].
- [8] Agilent HDMP 1032-1034 Transmitter-Receiver Chip-set Datasheet [<https://www.asc.ohio-state.edu/physics/cms/cfeb/datasheets/hdmp1032.pdf>].
- [9] ATLAS Collaboration, *ATLAS level-1 trigger: Technical Design Report*, ATLAS-TDR-12 [<https://cds.cern.ch/record/381429/>].